

Recruitment Timing and Dynamics of Transcription Factors at the *Hsp70* Loci in Living Cells

Katie L. Zobeck,^{1,4} Martin S. Buckley,^{1,4} Warren R. Zipfel,² and John T. Lis^{1,3,*}

¹Department of Molecular Biology and Genetics

²Department of Biomedical Engineering
Cornell University, Ithaca, NY 14853, USA

³Visiting Foreign Professor, Department of Biomedical Engineering, Dongguk University, Seoul, South Korea

⁴These authors contributed equally to this work

*Correspondence: jtl10@cornell.edu

DOI 10.1016/j.molcel.2010.11.022

SUMMARY

Chromatin immunoprecipitation (ChIP) studies provide snapshots of factors on chromatin in cell populations. Here, we use live-cell imaging to examine at high temporal resolution the recruitment and dynamics of transcription factors to the inducible *Hsp70* loci in individual *Drosophila* salivary gland nuclei. Recruitment of the master regulator, HSF, is first detected within 20 s of gene activation; the timing of its recruitment resolves from RNA polymerase II and P-TEFb, and these factors resolve from Spt6 and Topo I. Remarkably, the recruitment of each factor is highly synchronous between different cells. In addition, fluorescence recovery after photobleaching (FRAP) analyses show that the entry and exit of multiple factors are progressively constrained upon gene activation, suggesting the gradual formation of a transcription compartment. Furthermore, we demonstrate that poly(ADP-ribose) (PAR) polymerase activity is required to maintain the transcription compartment. We propose that PAR polymers locally retain factors in a transcription compartment.

INTRODUCTION

A variety of cellular signals trigger the recruitment of transcription factors (TFs) to specific target genes, allowing for a myriad of biochemical processes that are required for high-level transcription. Our knowledge of these processes has been guided mainly by biochemical techniques, including chromatin immunoprecipitation (ChIP), that assay when, where, and to what levels TFs are associated with specific regions of the DNA. These spatial and temporal resolution assays have provided important constraints for models of transcription mechanisms in vivo (Farnham, 2009; Saunders et al., 2006). However, most of these studies are restricted to assaying static images of chromatin-protein interactions in a population of cells. Recent advances in live-cell imaging technology allow for the real-time imaging of TFs at

specific loci in single cells, providing new insights into gene regulation (Hager et al., 2009).

Drosophila salivary glands offer a unique platform to carry out live-cell imaging studies of transcription (Lis, 2007). Salivary gland nuclei contain polytene chromosomes, comprised of thousands of aligned DNA strands showing packing similar to interphase diploid nuclei (Beerermann, 1972). This natural amplification allows for the imaging of the localization and dynamics of TFs at specific native loci in single cells (Yao et al., 2006, 2007, 2008).

Heat shock (HS) results in decondensation of transcriptionally activated chromatin at the *Hsp70* loci that are visualized as a discrete pair of puffs on polytene chromosomes (Ritossa, 1962). These two cytological loci, 87A and 87C, are 3D structures that contain two and four copies of *Hsp70*, respectively, as well as intervening DNA and a large spectrum of nuclear proteins. Studies of the distribution of specific proteins before and after HS have provided key insights into their function at the *Hsp70* loci (Fuda et al., 2009; Gilmour, 2009; Saunders et al., 2006). Importantly, many of the proteins identified as involved in *Hsp70* gene regulation have corresponding roles at other genes and in a variety of organisms, indicating their functions during transcription are evolutionarily conserved (Saunders et al., 2006).

HS induction leads to the recruitment of the transcription activator, heat shock factor (HSF), which trimerizes and binds to the regulatory regions of HS genes (Guertin and Lis, 2010; Lis and Wu, 1993; Perisic et al., 1989). Both fixed-cell analyses (Westwood et al., 1991) and more recent live-cell imaging have shown that HSF-eGFP resides in the nucleoplasm and is recruited to many chromosomal sites, including the *Hsp70* loci upon HS (Yao et al., 2006). Fluorescence recovery after photobleaching (FRAP) for transcription activators of different genes has shown dynamic associations with the chromatin (Hager et al., 2009). In contrast, upon HS, HSF stably associates with active *Hsp70* loci to form a platform for programming many rounds of RNA polymerase II (Pol II) transcription before dissociating from the locus (Yao et al., 2006).

Interestingly, even before HSF binds, Pol II is transcriptionally engaged but paused at the 5' end of the *Hsp70* gene. After HS, the paused Pol II escapes into active elongation, and additional Pol II is recruited to the gene (Rougvie and Lis, 1988). Live-cell imaging studies of Pol II have provided insights into the

molecular dynamics of a transcribing locus. Intriguingly, eGFP-Pol II reaches maximum fluorescence intensity at the *Hsp70* loci after its association with chromatin reaches saturation as measured by ChIP (Yao et al., 2007). Additionally, FRAP assays show a dramatic change in the local dynamics of eGFP-Pol II at *Hsp70* loci after activation. During the early stages of HS (20 min HS), eGFP-Pol II recovers completely over the course of 2 min after FRAP, at a rate consistent with the elongation rate; however, after 40–60 min of HS, little or no recovery is observed, even though transcription continues (Yao et al., 2007). Together, these studies provide evidence for the accumulation of Pol II at transcriptionally active loci followed by progressive retention and recycling of Pol II over the course of activation. The accumulation and progressive retention of Pol II at the *Hsp70* loci has been termed a transcription compartment and is postulated to provide a mechanism for the recycling of Pol II to allow continued rounds of transcription (Yao et al., 2007). It has been hypothesized that poly(ADP-ribose) (PAR) polymers form the HS puff structure and may be a means to locally retain factors at the loci (Tulin and Spradling, 2003). Interestingly, previous studies have shown that PAR polymerase (PARP), an enzyme that catalyzes the formation of PAR polymers, is required for HS puff formation (Tulin and Spradling, 2003), and PARP is involved in the rapid loss of nucleosomes at *Hsp70* genes upon activation (Petesch and Lis, 2008). However, the importance PARP activity for the local retention of factors in a transcription compartment has not been tested.

Transcriptional activation of the *Hsp70* genes by HS results in the recruitment of numerous TFs, including P-TEFb, Spt6, and topoisomerase I (Topo I) (Andrulis et al., 2000; Gilmour et al., 1986; Kaplan et al., 2000; Lis et al., 2000). P-TEFb is a kinase responsible for phosphorylating the C-terminal domain (CTD) of Pol II to permit Pol II's escape into active elongation (Marshall et al., 1996). P-TEFb is composed of CycT and Cdk9 and localizes to the 5' end as well as the entire transcribed region of *Hsp70* after HS (Boehm et al., 2003; Peterlin and Price, 2006). Spt6 is a nucleosome chaperone (Bortvin and Winston, 1996), known to be recruited to the nucleosome-containing region of the gene upon activation, and is notably absent from the 5' end of the gene, which is free of nucleosomes (Ni et al., 2008; Saunders et al., 2003). Topo I is recruited to remove supercoils generated by transcription (Wang, 2002) and is strongly recruited to the *Hsp70* loci upon activation (Fleischmann et al., 1984). It has been identified as a hyperphosphorylated CTD-interacting protein (Carty and Greenleaf, 2002) and, like Spt6, associates with the nucleosome-containing region as opposed to the 5' end (Gilmour et al., 1986; Kroeger and Rowe, 1992). Even though these factors bind to different regions of the *Hsp70* gene, ChIP studies done after different lengths of HS show they are all rapidly recruited upon activation (Boehm et al., 2003; Ni et al., 2008); however, these studies are not of sufficient temporal resolution to resolve their order of recruitment.

In this study, we examined the recruitment of the transcription activator HSF, RNA polymerase Pol II, and the elongation factors P-TEFb, Spt6, and Topo I to the native *Hsp70* loci with unprecedented temporal resolution in living cells. Our studies resolve the recruitment timing of these factors, providing temporal information that sets limits for their functional roles, and identify a

strikingly synchronous recruitment among different cells of these factors upon activation. We also assess the fate of histone H2B and PARP at the *Hsp70* loci after activation and chromatin decondensation. Then, using FRAP, we test the possibility that these factors are progressively retained in a transcription compartment that forms over extended gene activation. Finally, we test the importance of PARP activity for retention of Pol II in the transcription compartment.

RESULTS

Localization of TFs with Pol II at Active Transcription Loci in Living Cells

Activation of the *Hsp70* genes leads to the decondensation of the chromatin at the *Hsp70* loci (87A&C) and concomitant recruitment of Pol II to these sites. In both fixed-chromosome spreads and intact living nuclei, these sites are the only doublet of Pol II "puffs" within HS nuclei and unambiguously identify the *Hsp70* loci (Jamrich et al., 1977; Yao et al., 2006). ChIP and immunostaining of polytene squashes have also shown that many TFs colocalize at the *Hsp70* loci after HS (Lis, 2007). We selected key factors involved in different aspects of the transcription elongation, P-TEFb, Spt6, and Topo I, and examined their localization patterns and recruitment to the *Hsp70* loci in vivo. To do this, we generated *Drosophila* transgenic lines that express a fluorescent protein (FP) (either eGFP or mRFP)-tagged TF and the complementary FP tagged on the Rpb3 subunit of Pol II, within third instar larva salivary glands. Laser scanning confocal microscopy (LSCM) was used to identify their location before and after HS activation in living cells.

LSCM shows that FP-tagged P-TEFb, Spt6, and Topo I are primarily localized within the nucleus before and after HS. More specifically, we observed colocalization between all three factors and FP-tagged Pol II at developmentally regulated loci in non-heat-shocked (NHS) nuclei (Figures 1A–1C and S1A–S1C). After a 20 min HS, the factors are depleted from the developmental loci and now colocalize with Pol II at the HS loci, including the two *Hsp70* loci (Figures 1D–1F and S1D–S1F). These colocalization results concur with previous immunofluorescence studies on squashed polytene chromosomes (Andrulis et al., 2000; Fleischmann et al., 1984; Kaplan et al., 2000; Lis et al., 2000) and confirm the recruitment of these factors to the *Hsp70* loci upon HS in living cells. Notably, these TFs are not detected at the *Hsp70* loci before HS (note the absence of signal for the *Hsp70* loci during NHS), unlike Pol II, which is present at these sites at low levels before HS. Additionally, consistent with what was seen previously in squashed polytene chromosomes (Fleischmann et al., 1984; Muller et al., 1985), we observe a strong recruitment of eGFP-Topo I to the nucleolus upon HS in living salivary glands.

Differences in the Timing and Rates of Recruitment among TFs

Figure 1 shows that mRFP-P-TEFb, eGFP-Spt6, and eGFP-Topo I are recruited to the *Hsp70* loci before 20 min HS. However, the precise timing and rate of this recruitment could differ, distinguishing two possible mechanisms, whereby TFs are simultaneously corecruited upon activation or where they are recruited

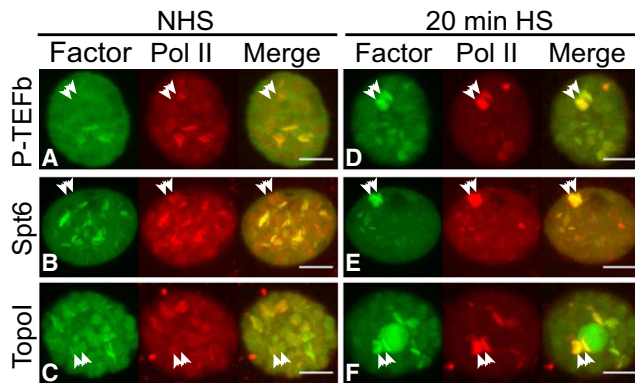


Figure 1. Colocalization of P-TEFb, Spt6, and Topo I with Pol II at Developmental and *Hsp70* Loci in Living Polytene Nuclei

(A–F) LSCM maximum intensity projections of polytene nuclei coexpressing mRFP-P-TEFb (A and D, left panel) and eGFP-Pol II (A and D, middle panel), eGFP-Spt6 (B and E, left panel) and mRFP-Pol II (B and E, middle panel), and eGFP-Topo I (C and F, left panel) and mRFP-Pol II (C and F, middle panel). (A)–(C) were imaged under NHS conditions, and (D)–(F) are the same nuclei imaged 20 min after HS. Merge is presented in right panel. Arrows highlight the position of the *Hsp70* loci. Scale bars are 10 μm . See also Figure S1.

in ordered, temporally and kinetically distinct steps. To achieve sufficient temporal resolution, we used spinning disk confocal microscopy (SDCM) because it provides faster data acquisition than LSCM. 3D image stacks were collected in both green and red channels during NHS using a 40 \times oil immersion objective maintained at room temperature. HS was activated by swapping in a matched objective heated to 36 $^{\circ}\text{C}$. The large heat capacity of the lens causes a nearly instantaneous HS (Yao et al., 2007) when the immersion medium contacts the coverslip ($t = 0$ s). Then, after adjusting for any changes in the focal plane, we obtained a time series consisting of two-channel 3D image stacks for 20 min at time intervals of 20–30 s (Figure 2A and Experimental Procedures). As previously seen (Yao et al., 2007), activation of the *Hsp70* genes does not result in a relocation of the *Hsp70* loci.

By imaging pairs of FP-tagged TFs, we are able to measure both the timing and rate of recruitment for both factors in the same nucleus. We measured the recruitment in the fly lines shown in Figure 1, as well as a line expressing HSF-eGFP, the activator of *Hsp70* transcription. The recruitment data for each factor were averaged using consecutive 10 s windows for both the mean intensity (Figure 2B) and the total intensity measurement (Figure 2C). Remarkably, the recruitment of HSF is detectable within 20 s after HS, while the recruitment of Pol II and the three other TFs occurs considerably later (>100 s after HS). Notably, HSF mean intensity decreases around 100 s after HS, while HSF total intensity plateaus at this time. Together with the observation that the *Hsp70* loci increase in volume with Pol II recruitment (Figure S2A), these results suggest that the decrease in HSF mean intensity is due to chromatin decondensation, not its dissociation from the loci.

To quantify reproducible differences in the initial timing of recruitment, we fit paired data sets with exponential curves and calculated the difference in recruitment times (Δt) for the

TF and Pol II to reach the same normalized fluorescence intensity. Because HSF was not imaged with Pol II in the same cell, we used a random sample of Pol II curves to calculate the pairwise differences in timing of recruitment. The time of initial recruitment, relative to Pol II, can be observed as the mean fluorescent intensities approach zero (Figures 2D–2G). We report all measurements averaged over multiple samples along with the standard error of the mean. If the TF is recruited faster than Pol II, the curve will slope to the left; if it is recruited slower, it will slope to the right. HSF is recruited 82 ± 5 s before Pol II. In contrast, P-TEFb is initially recruited around the same time as Pol II (1 ± 6 s after Pol II), and Spt6 and Topo I are recruited after Pol II (12 ± 4 and 22 ± 5 s after Pol II, respectively).

The recruitment data also provide the rates of recruitment to the *Hsp70* loci (Figure S2B), as assessed by fitting the data to a single exponential curve. The rate of HSF recruitment is much faster than the rate for either Pol II or the three elongation factors; this was also observed in Figure 2D by the curve sloping to the left. Additionally, the rates of recruitment for P-TEFb and Topo I are significantly slower than Pol II (Figures S2B, 2E, and 2G). Spt6, however, has a rate that is indistinguishable from Pol II (Figures S2B and 2F), suggesting a proportional recruitment of these two factors. These differences in timing and rates of recruitment for the different TFs demonstrate a sequential and independent recruitment of these factors to the *Hsp70* loci rather than a concerted corecruitment of factors, supporting the view that each factor has its own mechanism and cue for recruitment.

Synchrony in the Recruitment of TFs to *Hsp70* Loci

Boettiger and Levine (2009) identified two patterns of developmental gene activation within *Drosophila* embryos: a stochastic activation of transcription, where the first detection of transcripts in different cells occurred over a range of 15–20 min, and a synchronous activation of transcription, where transcripts in cells are detected within a 3 min range. This synchronous activation is hypothesized to facilitate the homogeneous expression of genes vital for proper development. Similarly, the coordinated and rapid activation of HS genes may be required to survive HS (O'Brien and Lis, 1993). Our time-lapse recruitment data provide a way to assess whether the recruitment of FP-tagged HSF, Pol II, P-TEFb, Spt6, and Topo I to the *Hsp70* loci occurs in a synchronous or stochastic manner in individual salivary gland nuclei. To assess the recruitment method, we compared the recruitment curves from nuclei within the same salivary gland as well as different salivary glands.

In all nuclei, HSF is recruited to the *Hsp70* loci rapidly after HS, and the initial recruitment is already observed by the first time point after HS (Figures 3A and S3A). Both the recruitment rates and times show little variation, reported here as standard errors, for nuclei in the same or from different glands, with the recruitment of HSF occurring 17 ± 1 s after HS. These data indicate rapid and highly synchronous recruitment. The recruitment times of Pol II following HS also show little variation, 103 ± 2 s (Figure 3B). Additionally, the recruitment times of the three TFs, P-TEFb, Spt6, and Topo I, are similarly restricted, 95 ± 3 , 115 ± 2 , and 132 ± 4 s, respectively (Figures 3C–3E and S3). Therefore, all five factors are recruited to *Hsp70* in a synchronous manner.

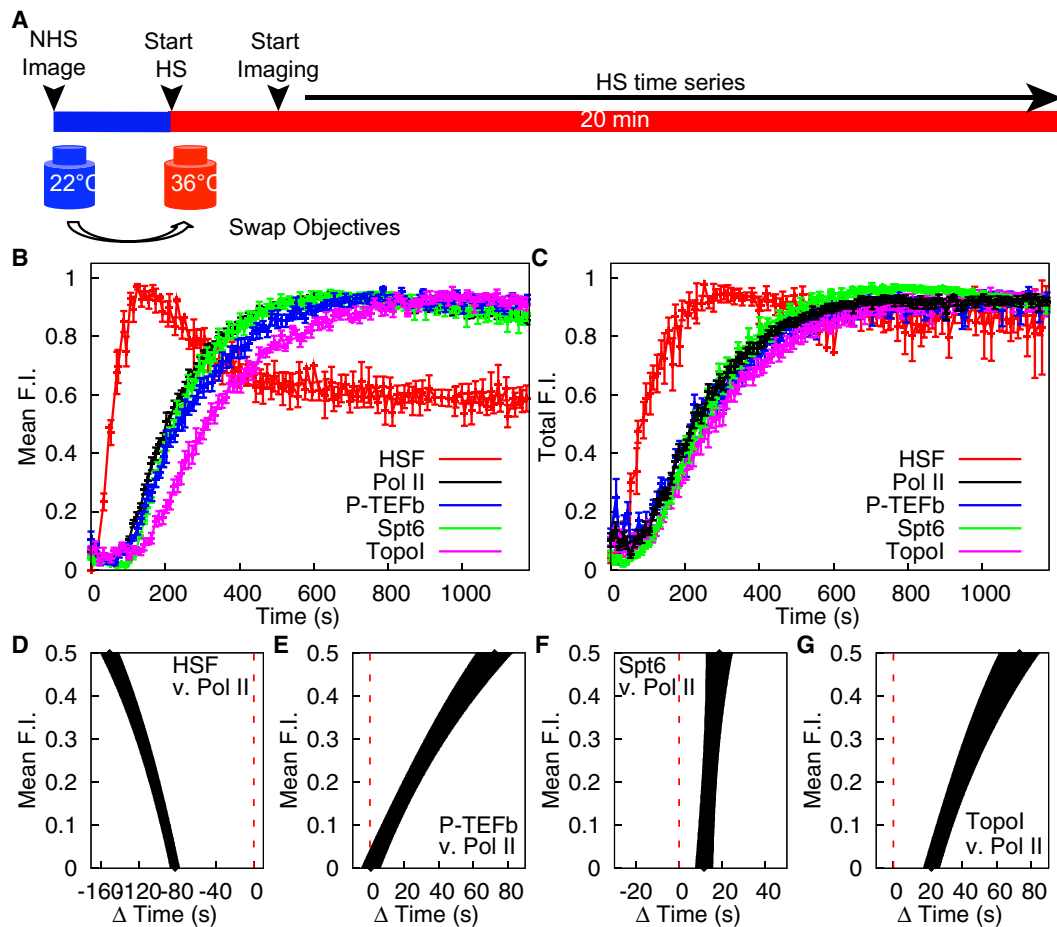


Figure 2. Recruitment Timing of TFs

(A) SDCM was used to obtain 3D images of FP-tagged TFs with the complementary FP-tagged Pol II. First, *Drosophila* salivary glands were imaged using a room temperature objective, then an objective preheated to 36°C was swapped in, causing a nearly instantaneous HS. 3D time series were then obtained continuously over 20 min.

(B and C) Normalized TF fluorescence intensities (F.I.) were averaged using 10 s windows using mean F.I. (B) and using total F.I. (C). HSF is in red, Pol II in black, P-TEFb in blue, Spt6 in green, and Topo I in purple. Number of samples (n) = 10, 32, 10, 12, and 10, respectively.

(D–G) Reproducible differences in recruitment times relative to Pol II were calculated by fitting exponential curves to each set of recruitment data for each factor: HSF (D, n = 10), P-TEFb (E, n = 10), Spt6 (F, n = 12), and Topo I (G, n = 10). Times to reach a specific intensity were calculated and subtracted from the times for Pol II from the same nucleus. Because HSF was not imaged with Pol II, a random set of Pol II curves was used to calculate the paired differences. The red dotted line at $\Delta t = 0$ represents the time Pol II reaches the corresponding intensity. Error bars represent the SEM. See also Figure S2.

Effect of HS Activation on the Localization of Histone H2B and PARP

Upon HS, dramatic structural changes occur at the *Hsp70* loci, which are visible in polytene chromosomes as the formation of a transcriptionally active puff (Ritossa, 1962). We have observed that the decondensation of the chromatin led to the observed decrease in mean fluorescence intensity of HSF, while the total fluorescence intensity remained constant (Figures 2B and 2C). Because HS activation leads to nucleosome loss at the *Hsp70* gene, via a rapid and transcription-independent and a slower transcription-dependent loss (Petesch and Lis, 2008), we wanted to address whether histones remain associated with the *Hsp70* loci during HS.

To address this possibility, we measured both the mean and total fluorescence intensity of mRFP-H2B at the *Hsp70* loci. We

observed that the mean fluorescence intensity decreases over time at the *Hsp70* loci (Figures 4A and 4C). However, to address whether histones (1) are physically lost from the loci or (2) stay associated with the loci but decrease in intensity due to chromatin decondensation, we measured the total intensity of H2B at the *Hsp70* loci using a constant volume defined by the maximum size of the *Hsp70* loci. Interestingly, the total fluorescence intensity remains constant, suggesting that H2B remains associated with loci after HS activation and chromatin decondensation (Figure 4E), even though in this time frame, nucleosome structure is disrupted at the *Hsp70* loci (Petesch and Lis, 2008).

Decondensation of the HS loci as well as the loss of nucleosome structure at *Hsp70* genes upon activation is dependent on PARP (Petesch and Lis, 2008), an enzyme that catalyzes the polymerization of ADP-ribose units from NAD⁺ (Kraus and

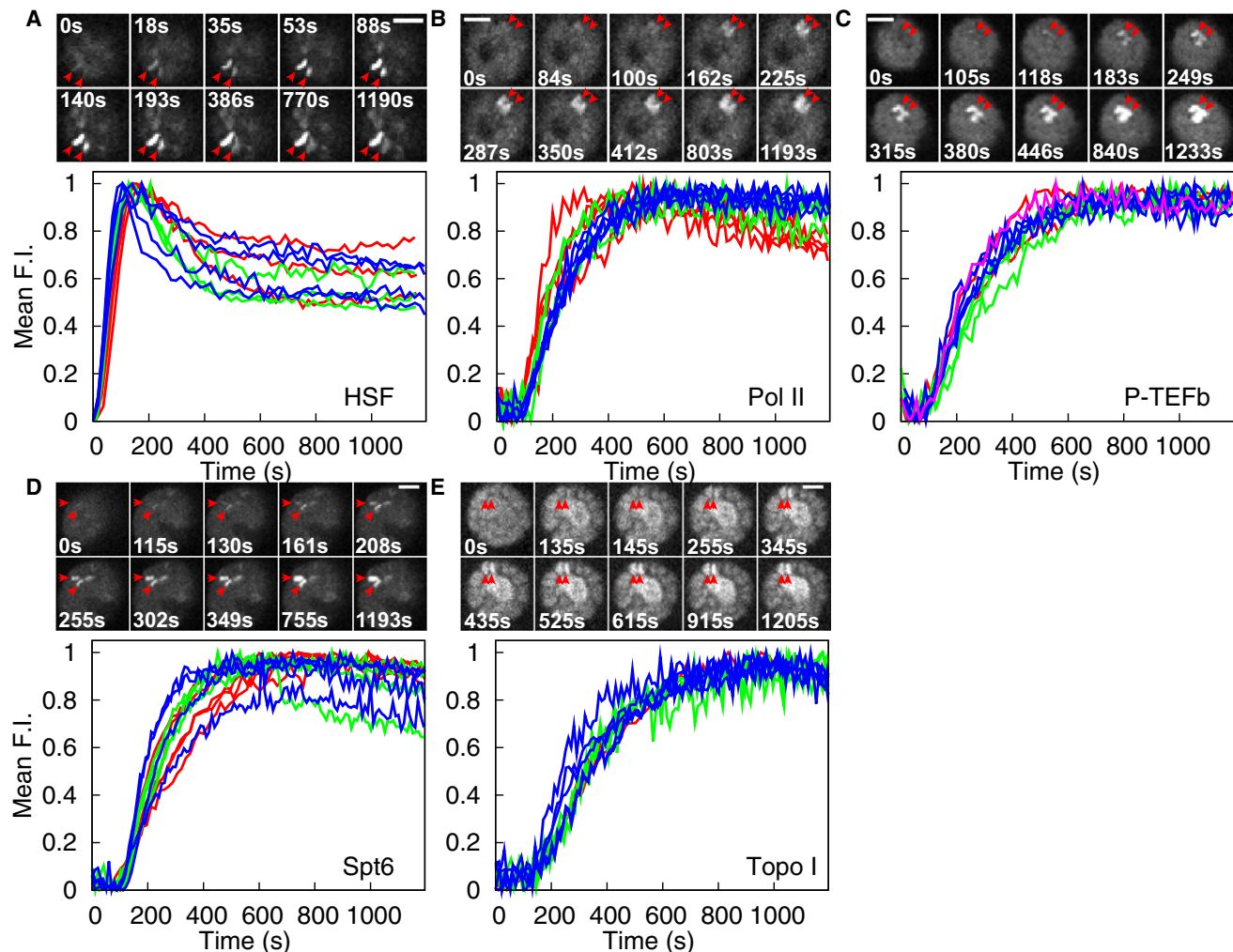


Figure 3. Synchrony in the Recruitment of TFs to *Hsp70* Loci among Nuclei of the Same Gland or in Different Glands

(A–E) Representative SDCM recruitment images and corresponding mean F.I. recruitment plots for mRFP-HSF (A), Pol II (mRFP and eGFP) (B), mRFP-P-TEFb (C), eGFP-Spt6 (D), and eGFP-Topo I (E). The first image for each factor is the NHS image and the second image is the time point before recruitment, while the rest of the images are spaced to depict the recruitment kinetics of the factors (note: HSF is recruited by the first time point after HS). Scale bars are 10 μ m. Plots show normalized mean F.I. of factors' recruitment in nuclei of the same gland (same color lines) and nuclei from different glands (different color lines) over 20 min HS. Each graph represents recruitment data from three or more glands containing two or more nuclei from each gland. Red arrows mark the location of the *Hsp70* loci. See also Figure S3.

Lis, 2003). In *Drosophila*, polytene squashes have shown that both PARP and PAR localize to the *Hsp70* loci upon activation (Tulin and Spradling, 2003). Therefore, using the same methods as for H2B, we measured the mean fluorescence intensity of PARP-eGFP over the course of HS and observed a decrease in intensity, similar to H2B (Figures 4B and 4D). However, measuring the total intensity of PARP (Figure 4F) revealed no large changes in total PARP intensity, suggesting that PARP, like H2B, remains associated with the *Hsp70* loci at a similar level before and after decondensation.

TFs Progressively Retained in Transcription Compartment over Time Course of HS

The FP-tagged TFs provide a means of examining not only their recruitment, but also their dynamics of association with

the *Hsp70* loci. For example, 10 min after HS, FRAP of eGFP-Pol II shows a complete and linear recovery of fluorescence that reflects the entry of new fluorescent Pol II onto the gene. In contrast, continued HS causes the progressive decrease in both the rate and total recovery of Pol II, even though transcription remains robust. This observation has been attributed to the progressive retention of Pol II in a transcription compartment that allows the recycling of Pol II for continued rounds of transcription (Yao et al., 2007). To address the possibility that this compartment is a more general feature of active transcription, we examined (1) whether there is an accumulation of FP-tagged factors beyond the amount needed to maximally bind the genes and (2) if the dynamics of representative TFs, P-TEFb, Spt6, and Topo I also change with the duration of HS.

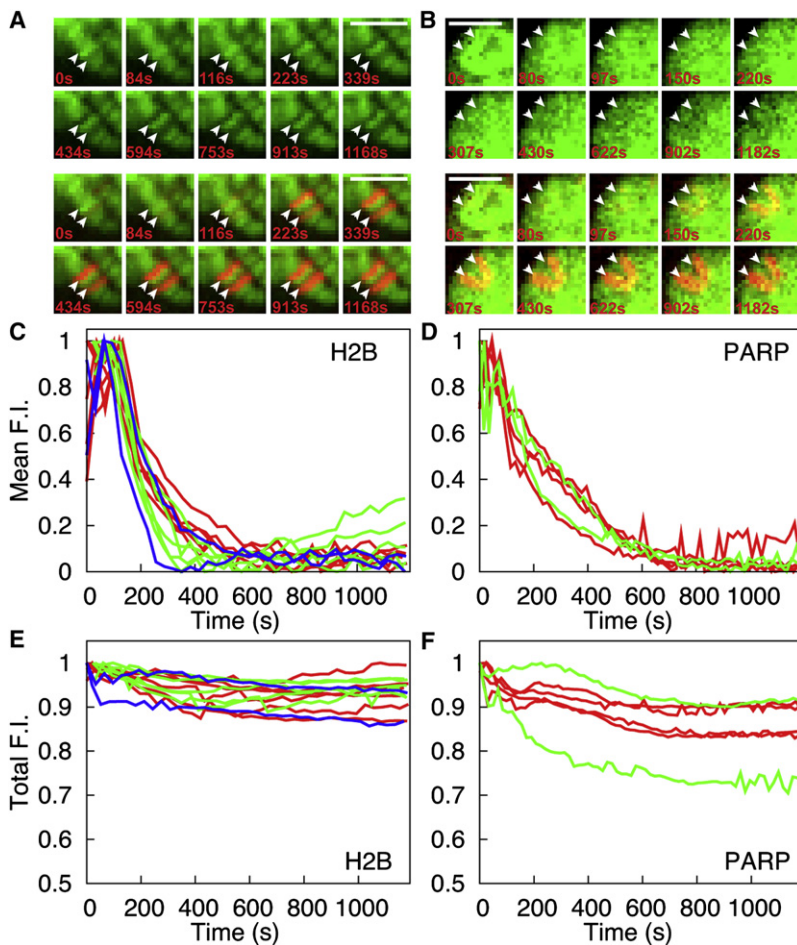


Figure 4. Association of H2B and PARP with *Hsp70* Loci after Decondensation

(A and B) Representative time course images illustrating the localization of mRFP-H2B (A) and PARP-eGFP (B) to the *Hsp70* loci after HS. Top panel shows the localization of the factor, while the bottom panel shows a merge between the factor (green) and Pol II (red). The first image (0 s) of each panel is the NHS image, the second image is the time point before additional Pol II recruitment, and consecutive images are spaced out over the course of HS. Arrows indicate the *Hsp70* loci, and a progressive decrease in mRFP-H2B or PARP-eGFP intensity can be seen in these images. Scale bars are 10 μm.

(C and D) Mean F.I. plots of mRFP-H2B (C) and PARP-eGFP (D), using Pol II as an indicator for the volume of the *Hsp70* loci. Lines of the same color are from the same gland, while different colors are from different glands. Two or three glands containing 2–4 nuclei each are plotted.

(E and F) Total F.I. plots using a constant volume for mRFP-H2B (E) and PARP-eGFP (F). Lines of the same color are from the same gland, while different colors are from different glands. Fluorescence intensity of 2–4 nuclei each from two or three glands are plotted for each factor.

First, we have compared the time for maximum recruitment to the *Hsp70* loci (Figure S3) and to the *Hsp70* genes (Figures S4A–S4C). Our high-resolution recruitment assay and salivary gland ChIP of Pol II on *Hsp70* (Figures S3 and S4A) agrees with the previous report that Pol II reaches maximum intensity at the loci after maximum binding has occurred on the gene (Boehm et al., 2003; Yao et al., 2007). We observe maximum levels at ~3 min HS for chromatin by ChIP (Figure S4A) and ~8 min HS at the locus by live-cell imaging (Figure S3B). Salivary gland ChIP experiments for the TFs P-TEFb and Spt6 also show maximal gene occupancy by ~3 min (Figures S4B and S4C), while they continue to accumulate at the *Hsp70* loci, achieving maximum total intensity at 10 and 8 min, respectively (Figures S3C and S3D). This suggests that there is an accumulation of TFs at the *Hsp70* loci beyond what is required to saturate the DNA.

Second, we examined whether the dynamics of these factors change with the duration of HS using FRAP. All FRAP experiments were done during recruitment equilibrium, where mean and total intensities of the TF are constant over time (Figures 5 and S4D–S4F). At 10 min HS, shortly after reaching recruitment equilibrium, the FRAP profile provides critical information regarding the dynamics of association between the factor and

the *Hsp70* loci. The one-half max ($\tau_{1/2}$) recovery time can be used to identify whether recovery is limited by the dissociation of the pre-existing bleached factors from their targets of interaction, i.e., a binding event, or if recovery is limited to diffusion (Sprague and McNally, 2005). For mRFP-P-TEFb, eGFP-Spt6, and eGFP-Topo I, the estimated $\tau_{1/2}$ for diffusion is less than 0.030 s, while the observed $\tau_{1/2}$ for these factors are 30, 40, and 10 s, respectively (Figures 5D,

5E, and 5F). This result indicates that these TFs are in fact binding at the *Hsp70* loci.

Because P-TEFb, Spt6, and Topo I are Pol II-interacting proteins (Fleischmann et al., 1984; Ni et al., 2008; Yoh et al., 2007), we also compared their recovery curves to Pol II to see if any of these three factors were stably binding to Pol II. If a stable interaction exists, we expect the FRAP dynamics to mimic that of Pol II. At early times of HS, 10–20 min, Pol II recovers from photobleaching linearly for 2 min. This recovery corresponds to the time it takes bleached Pol II molecules to complete transcription elongation and for new fluorescent Pol II to refill the gene (Yao et al., 2007). The recovery curves for the three TFs are all exponential, indicating that these three TFs are not stably bound to Pol II, but instead interact transiently with Pol II or the *Hsp70* loci.

Prolonged HS also impacted the FRAP dynamics of the three TFs at the *Hsp70* loci. The most dramatic effect was seen with Spt6, which recovers to 50% initial intensity after a 10 min HS. However, after a 20 min HS, less recovery is observed, and after 40 min HS, no recovery is observed after FRAP (Figures 5B and 5E). Figure S4 confirms Spt6 is present at similar intensities at all of these time points. Together, these results indicate that Spt6 becomes more stably associated with the *Hsp70* loci with increasing HS time, and these findings are consistent with this

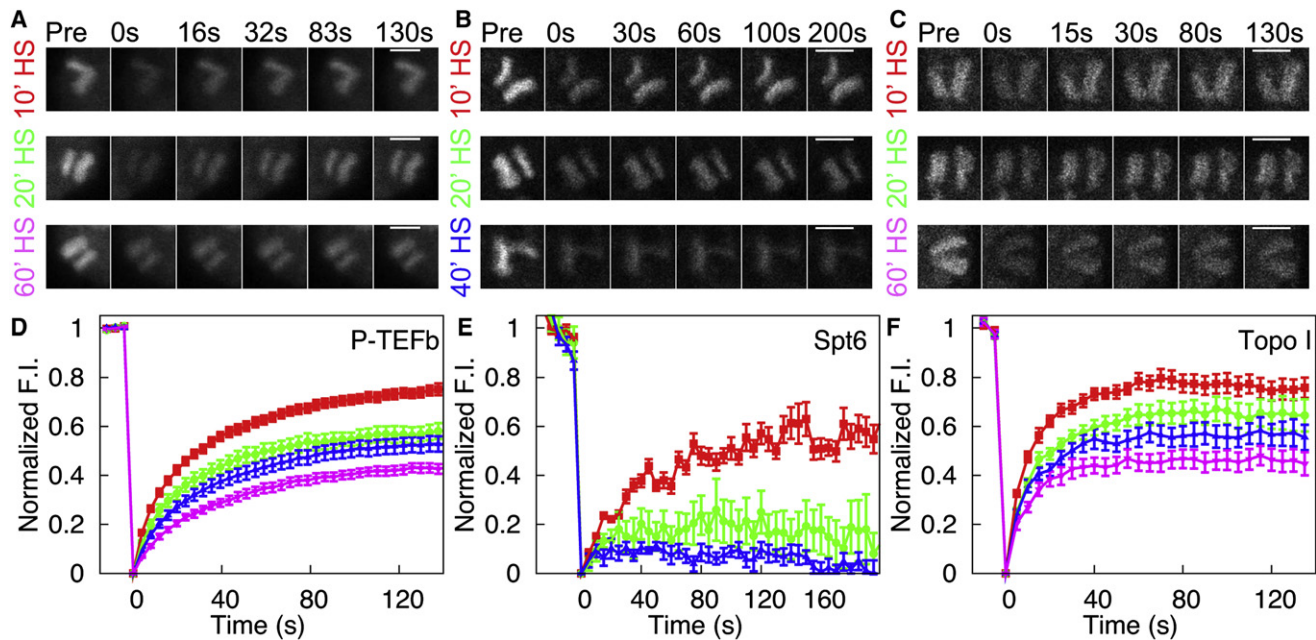


Figure 5. FRAP Dynamics of TFs at the *Hsp70* Loci Change after Length of HS

(A–C) FRAP of the three TFs after different lengths of HS: mRFP-P-TEFb (A), eGFP-Spt6 (B), and eGFP-Topo I (C). Panels show representative FRAP images. The top panel was bleached after 10 min HS, middle panel was bleached after 20 min HS, and lower panel was bleached after 40 min HS (B) or 60 min HS (A and C). All scale bars equal 10 μ m.

(D–F) Plots of normalized F.I. at the *Hsp70* loci: mRFP-P-TEFb (D), eGFP-Spt6 (E), and eGFP-Topo I (F). Bleaching resulted in a decrease of 40%–60% initial F.I.; however, these plots are normalized to both initial F.I. and bleach depth. Red, 10 min HS; green, 20 min HS; blue, 40 min HS; purple, 60 min HS ($n = 11, 10, 12,$ and 10 for P-TEFb, respectively; $n = 13, 6,$ and 6 for Spt6, respectively; $n = 13, 20, 17,$ and 16 for Topo I, respectively). Error bars represent the SEM. See also Figure S4.

factor, which is required for maximum transcription elongation rates (Ardehali et al., 2009), being reused and recycled within the compartment.

In contrast to Spt6, Topo I and P-TEFb remain dynamic during prolonged HS. However, increasing HS time still causes a progressive decrease in the mobile fraction of Topo I and P-TEFb, such that the immobile fractions of both Topo I and P-TEFb reach 60% of the total population in the 60 min HS sample (Figures 5A, 5C, 5D, and 5F). The increase in the immobile fraction observed for these two factors could be explained in a similar manner as Spt6, whereby the immobile fraction consists of an increasing number of molecules that can be recycled for use in transcription.

Together, our salivary gland ChIP results and FRAP dynamic studies suggest that the transcription compartment is a general feature of active transcription and is not limited to Pol II. Notably, our FRAP results emphasize that the compartmentalization process is not simply a mechanism by which TFs become completely retained at the loci after HS and suggest that differences in a TF's function, size, or affinity for the loci may play a role in the ability of a given TF to diffuse into or out of the compartment.

Role of PARP in Compartment Formation

Previous studies have shown that PAR chains accumulate at the *Hsp70* loci upon activation, and that the enzymatic activity of PARP, the enzyme that catalyzes PAR chain formation, is required for the structure of HS puff (Tulin and Spradling,

2003). Our study extends these findings to show that PARP continues to associate with the *Hsp70* loci upon activation. Based on these findings, we hypothesized that PARP catalytic activity is responsible for the retention of factors in the transcription compartment. To address this hypothesis, we tested the effect of specifically inhibiting PARP catalytic activity using the drug PJ34 on the compartmentalization of eGFP-Pol II, the defining factor of the transcription compartment (Yao et al., 2007), during late HS. The experimental setup is illustrated in Figure 6A. We heat shocked the glands for 35 min and then perfused 3 μ M PJ34 or media only over the glands for 5 min, after which we acquired FRAP curves. Perfusion does not affect the compartment behavior of Pol II when compared to a 40 min HS no-perfusion control (Figures 6B and 6D). Strikingly, PJ34 perfusion after 40 min HS has a drastic effect on the FRAP dynamics of Pol II, which now completely recovers over the course of 120 s (Figures 6B and 6C). This recovery is remarkably similar to the 10 min HS FRAP behavior of Pol II, indicating that PARP inhibition leads to a condition resembling the precompartment state. This result indicates that the catalytic activity of PARP is required for retaining Pol II in a compartment.

DISCUSSION

Recruitment Timing and Rates for TFs during HS

The *Drosophila Hsp70* genes provide a unique system with which to examine the recruitment of TFs to specific chromosomal loci.

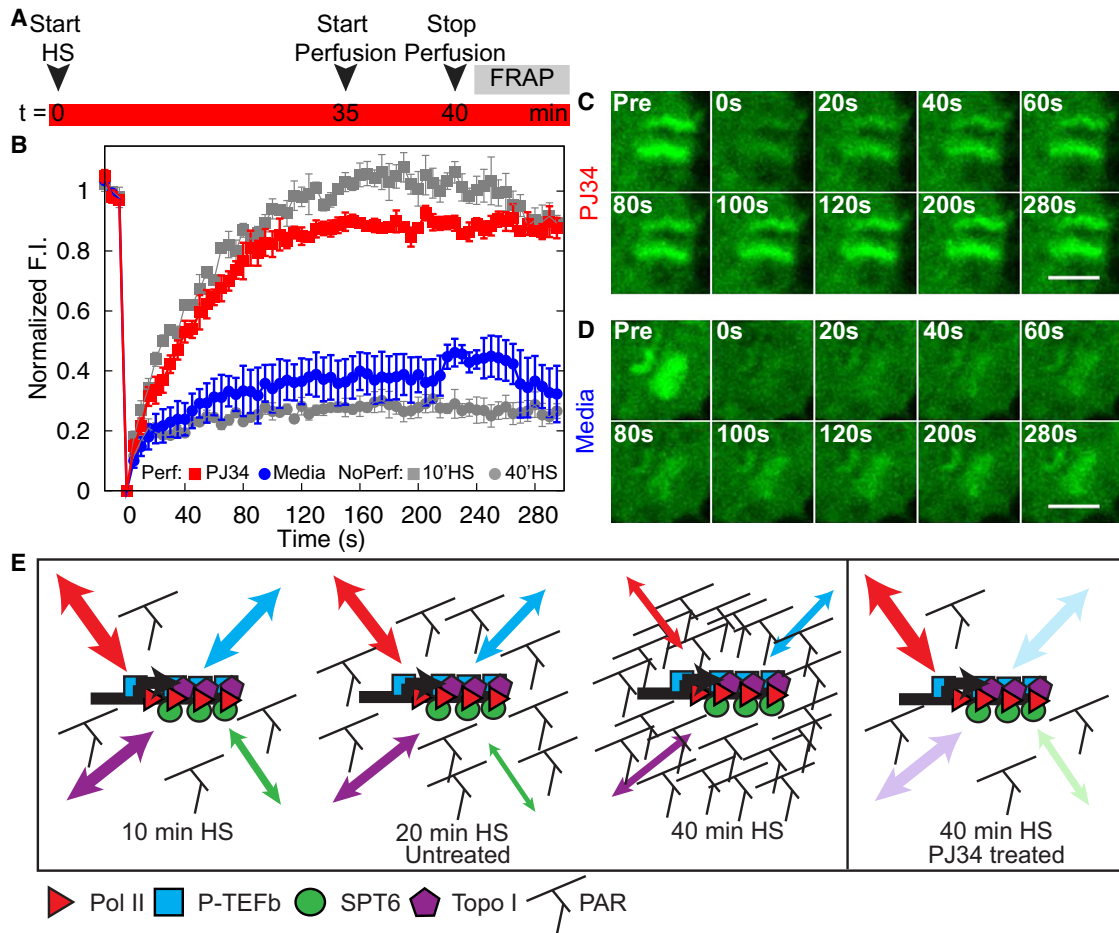


Figure 6. PARP Catalytic Activity Is Required for the Maintenance of the Transcription Compartment

(A) Schematic of PJ34 perfusion protocol. Media only or 3 μ M PJ34 was perfused over the gland for 5 min starting 35 min after HS. FRAP of eGFP-Pol II at the *Hsp70* loci was initiated as soon as perfusion stopped.

(B–D) FRAP of eGFP-Pol II in PJ34 perfused glands and controls. FRAP curves of eGFP-Pol II (B) were perfused with PJ34 (red, n = 3) at 40 min HS or with media only at 40 min HS (blue, n = 4) and no perfusion controls at 10 min HS (gray squares, n = 4) and 40 min HS (gray circles, n = 3). Error bars represent SEM. Representative images of eGFP-Pol II are shown after PJ34 perfusion (C) and after media-only perfusion (D). Scale bars = 5 μ m.

(E) Model for the progressive formation of transcription compartment during the time course of HS. PARylated proteins accumulate at the *Hsp70* loci over HS activation. The accumulation of PAR restricts the ability of proteins to diffuse into and out of the compartment, with individual factors behaving differently, with Spt6 and Pol II unable to exchange with the surrounding nucleoplasm by 40 min HS. Treatment with PJ34, a PARP inhibitor, at 40 min HS reduces the amount of PAR present and restores the ability of Pol II to exchange with the nucleoplasm. Light shaded arrows represent the potential dynamics of the TFs after PJ34 treatment.

They are rapidly and robustly activated upon HS and are located at two cytological loci, whose appearance provides a diagnostic doublet for identifying the *Hsp70* loci in living cells. By measuring the intensity of TFs at the *Hsp70* loci over the course of HS, we have been able to distinguish differences in the initial timing and rates of recruitment of TFs.

We have previously shown in a population of cells that HSF appeared to be recruited to the *Hsp70* genes before Pol II (Boehm et al., 2003); however, our present study shows this more convincingly at high temporal resolution and also demonstrates a sequential recruitment of the other factors, P-TEFb, Spt6, and Topo I, to the *Hsp70* loci rather than a concerted corecruitment of a preassembled transcription complex. In single cells, we observe that HSF is recruited 80 s before Pol II, suggesting

that other coactivators or modifications are required for Pol II recruitment. P-TEFb is first detected at *Hsp70* loci when Pol II also begins to increase, which is consistent with the P-TEFb kinase's role in promoting active elongation (Zhou et al., 2000). The recruitment of Spt6 follows 10 s after Pol II, which is consistent with the known role of Spt6 as a chromatin remodeler and the time for Pol II to reach the first nucleosome. Then Topo I, which interacts with the phosphorylated CTD of Pol II (Carty and Greenleaf, 2002), is recruited 20 s after Pol II and P-TEFb. Interestingly, this raises the possibility that Pol II phosphorylation is not sufficient to recruit Topo I, but rather that Topo I recruitment may require transcription-driven accumulation of supercoiled DNA (Madden et al., 1995). Finally, a model has been recently proposed where genes are recruited to nuclear sites

called transcription factories, which contain the TFs required for transcription and its regulation (Carter et al., 2008). The distinct kinetics observed here for the five TFs and the failure to see movement of the *Hsp70* loci within the nucleus in polytene nuclei upon activation (here and Yao et al., 2007) are inconsistent with *Hsp70* genes being recruited to a preformed transcription factory. Furthermore, we do not observe an increase in colocalization of the HS loci in diploid nuclei after HS (Yao et al., 2007).

Synchronous Recruitment of TFs

This study provides a single-cell analysis with the temporal resolution to address whether TFs are synchronously recruited to *Hsp70* loci. Our study revealed that HSF, Pol II, and three TFs (P-TEFb, Spt6, and Topo I) are each synchronously recruited to the *Hsp70* loci. We observed a standard error for each TF's recruitment timing to be less than 6 s. Interestingly, genes that have paused Pol II may in general be synchronously activated. Boettiger and Levine examined numerous development genes in early embryos at the level of RNA accumulation in cells and observed that genes containing a paused Pol II were synchronously activated (range of 3 min), while genes without a paused Pol II were stochastically activated (range of 20 min) (Boettiger and Levine, 2009).

We propose that the paused Pol II, present on *Hsp70* genes, may facilitate the synchronous recruitment of HSF by maintaining an open chromatin state at the promoter to provide the activator, HSF, with accessible binding sites. It has been shown that HSF binding to *Hsp70* transgenes depends on an open chromatin state that in turn requires GAGA factor and paused Pol II (Shopland et al., 1995). More generally, the paused/stalled Pol II at promoters has been shown to be important in keeping nucleosomes off promoters (Gilchrist et al., 2008). The open chromatin state may increase the probability of activator binding its target sequence (Tsukiyama et al., 1994). In addition, other factors may also gain more efficient access to genes that have a promoter-paused Pol II. The preassembled general TF complex at these promoters should facilitate binding and initiation of newly recruited Pol II following activation (Lebedeva et al., 2005). Synchronous recruitment of Pol II might then promote the synchronous recruitment of the other TFs and synchronous transcript accumulation. Importantly, these studies provide insights into a mechanism that ensures the rapid and uniform induction of the HS response that is vital to the viability of organisms under stress conditions.

Transcription Compartment

The transcription compartment has previously been defined by Pol II's progressive retention and recycling over extended times of gene activation (Yao et al., 2007). By comparing the times of maximum recruitment for the *Hsp70* loci and the *Hsp70* genes, we were able to show there is an accumulation of molecules at the loci beyond what can bind DNA. Then, using FRAP, we showed three TFs, CycT, Spt6, and Topo I, are also progressively retained at the *Hsp70* loci. These findings suggest that the transcription compartment is not limited to Pol II, but also involves the retention and perhaps recycling of other components of the transcription machinery.

Moreover, our results set further limitations on the structure of the compartment. In the case of Pol II (Yao et al., 2007) and Spt6 (Figure 5E), the FRAP recoveries progressively decrease until no recovery is observed. In contrast, a portion of P-TEFb and Topo I continue to exchange with the nucleoplasm even after an hour of HS, but over time, an increasing percentage of molecules remain stably associated with the locus. These different behaviors suggest that the transcription compartment is not a completely closed entity formed over time, but either an affinity-based retention or the formation of a porous barrier.

Affinity-based retention and porous barrier models are not mutually exclusive. PAR, which accumulates at the *Hsp70* and developmental loci in response to gene activation (Tulin and Spradling, 2003), could be the foundation of the porous barrier, but could also be responsible for the affinity-based retention of factors with strong nucleic acid affinity, as has been documented for histones (Althaus et al., 1994). To investigate these models, we assayed the role of PAR in compartment formation by using PJ34, a specific inhibitor of PARP catalytic activity (Garcia Soriano et al., 2001), and showed that the dynamics of Pol II at the *Hsp70* loci, 40 min after HS, return to the early HS dynamics upon PJ34 treatment. Inhibition of PARP prevents the polymerization of more PAR, which the PAR glycohydrolase (PARG) can now rapidly degrade (D'Amours et al., 1999). Thus, we suggest that PARG activity reduces the overall amount of PAR at the *Hsp70* loci and allows a remobilization of Pol II to the 10 min HS behavior. We hypothesize that the other factors will similarly be remobilized, and a thorough study of these factors and the formation and properties of the compartment requires a future concentrated study. Based on our results, we propose the model in Figure 6E, where extended HS activation leads to the accumulation of PAR chains at the *Hsp70* loci. Early on (10 min HS), the number or size of these chains is small enough that many proteins can easily diffuse into and out of the area. Some factors, like Spt6, however, may already be partially immobilized because of their affinity toward nucleic acids. Over time (20 min HS and then 40 min HS), the number of PAR chains increases at the *Hsp70* loci, reducing the ability of some factors (Topo I and CycT) to freely diffuse with the nucleoplasm and fully preventing the exchange of Spt6 and Pol II with the nucleoplasm, although they are able to be reused for continued rounds of transcription (Yao et al., 2007).

Finally, our study addresses whether histones remain associated with the *Hsp70* loci after activation and chromatin decondensation, and the results indicate surprisingly that H2B remains associated, even though upon activation the nucleosomes rapidly dissociate from the *Hsp70* genes (Petesch and Lis, 2008). Therefore, we suggest that the early transcription compartment may be involved in retaining H2B at the *Hsp70* loci. Additionally, our observation that PARP also remains associated with the *Hsp70* loci suggests that PARP might be a component of the compartment. However, further experiments are needed to test these hypotheses.

In conclusion, our kinetic analysis of TF recruitment and dynamics by live-cell imaging provides insights into the overall mechanics and architecture of the transcription loci. Future development of imaging technologies should provide the ability

to examine diploid cells and thereby address the conservation of these mechanisms in different cell types and organisms.

EXPERIMENTAL PROCEDURES

Spinning Disk Microscopy

Drosophila salivary glands, from the crosses described in the [Supplemental Experimental Procedures](#), were dissected from third instar larva as previously described (Yao et al., 2008) and transferred immediately with medium to a Mat-Tek glass-bottomed culture dish (P35G-1.0-14-C), and a glass coverslip was placed on top to reduce evaporation and movement of the glands. A Carl Zeiss Cell Observer SD system with the Yokogawa CSU-X1 spinning disk unit and a Hamamatsu C9100-13 EMCCD was used to obtain confocal 3D stacks with two channels and time intervals of 10–30 s. Two identical Plan-Apochromat 40×/1.3 Oil Iris objectives were used; one was maintained at room temperature and one was heated to 36°C using a Biopetechs Objective Heater. A 40 μm preactivation Z stack with 1 μm sections was taken using the room temperature objective in both channels, alternating channels every slice. Then, the 36°C objective was moved into position; HS times were started at the moment the objective contacted the slide. A xyzt series with 40 Z sections was obtained after readjusting the focal position. Time intervals were between 10 and 30 s, and the time series lasted 20 min (Figure 2A). Images were taken at a resolution of 512 × 512 pixels using 16-bit color depth. Details regarding data analysis can be found in the [Supplemental Experimental Procedures](#).

Laser Scanning Confocal Microscopy and Multiphoton Microscopy

Dissected glands were transferred with medium to a Biopetechs FCS3 Closed Chamber System with a 0.2 mm spacer. We used an upright confocal/multiphoton microscope system (Carl Zeiss LSM510 META). NHS images were obtained with a C-Apochromat 63×, 1.2 NA, water immersion objective. For HS, an identical objective was swapped in for the room temperature objective in the same manner as described above.

FRAP

Dissected glands were imaged using MPM as described above. Perfusion of 3 μM PJ34 or media alone into the FCS3 chamber occurred as depicted in Figure 6A. We used a circular ROI limited to the dimensions of the *Hsp70* loci. eGFP samples were photobleached with a Mai Tai laser (Spectra-Physics; Irvine, CA) at 910 nm with a power of 15–20 mW (measured after the objective). mRFP photobleaching used the same laser at 800 nm using 40–50 mW. These settings photobleached the samples to 40%–60% initial intensity. Images were corrected for acquisition photobleaching by monitoring a small nuclear region. FRAP curves were normalized for prebleach images to equal one, and first image after the bleach equal to 0. Recovery times were obtained by fitting the FRAP data to $f(t) = A \times (1 - C_{eq} \times e^{-k_{off} \times t})$ (Sprague et al., 2004).

SUPPLEMENTAL INFORMATION

Supplemental Information includes Supplemental Experimental Procedures, Supplemental References, and four figures and can be found with this article online at [doi:10.1016/j.molcel.2010.11.022](https://doi.org/10.1016/j.molcel.2010.11.022).

ACKNOWLEDGMENTS

We thank Nina Allen and Scott Olenych from the David H. Murdock Research Institute for use of the Carl Zeiss Cell Observer SD system and Tudor Marian for his generosity in writing the MatLab programs. This work was partly performed in the Developmental Resources for Biophysical Imaging Opto-Electronics and was supported by NIH grant GM25232 to J.T.L., NSF grant CHE-0242328 to W.W. Webb and J.T.L., and NIH grant GM087003 to M.S.B.

Received: February 24, 2010

Revised: May 20, 2010

Accepted: October 8, 2010

Published: December 21, 2010

REFERENCES

- Althaus, F.R., Höfner, L., Kleczkowska, H.E., Malanga, M., Naegeli, H., Panzeter, P.L., and Realini, C.A. (1994). Histone shuttling by poly ADP-ribosylation. *Mol. Cell. Biochem.* **138**, 53–59.
- Andrulis, E.D., Guzmán, E., Döring, P., Werner, J., and Lis, J.T. (2000). High-resolution localization of *Drosophila* Spt5 and Spt6 at heat shock genes in vivo: roles in promoter proximal pausing and transcription elongation. *Genes Dev.* **14**, 2635–2649.
- Ardehali, M.B., Yao, J., Adelman, K., Fuda, N.J., Petesch, S.J., Webb, W.W., and Lis, J.T. (2009). Spt6 enhances the elongation rate of RNA polymerase II in vivo. *EMBO J.* **28**, 1067–1077.
- Beermann, W. (1972). Chromomeres and genes. *Results Probl. Cell Differ.* **4**, 1–33.
- Boehm, A.K., Saunders, A., Werner, J., and Lis, J.T. (2003). Transcription factor and polymerase recruitment, modification, and movement on dhsp70 in vivo in the minutes following heat shock. *Mol. Cell. Biol.* **23**, 7628–7637.
- Boettiger, A.N., and Levine, M. (2009). Synchronous and stochastic patterns of gene activation in the *Drosophila* embryo. *Science* **325**, 471–473.
- Bortvin, A., and Winston, F. (1996). Evidence that Spt6p controls chromatin structure by a direct interaction with histones. *Science* **272**, 1473–1476.
- Carter, D.R., Eskiw, C., and Cook, P.R. (2008). Transcription factories. *Biochem. Soc. Trans.* **36**, 585–589.
- Carty, S.M., and Greenleaf, A.L. (2002). Hyperphosphorylated C-terminal repeat domain-associating proteins in the nuclear proteome link transcription to DNA/chromatin modification and RNA processing. *Mol. Cell. Proteomics* **1**, 598–610.
- D'Amours, D., Desnoyers, S., D'Silva, I., and Poirier, G.G. (1999). Poly(ADP-ribosylation) reactions in the regulation of nuclear functions. *Biochem. J.* **342**, 249–268.
- Farnham, P.J. (2009). Insights from genomic profiling of transcription factors. *Nat. Rev. Genet.* **10**, 605–616.
- Fleischmann, G., Pflugfelder, G., Steiner, E.K., Javaherian, K., Howard, G.C., Wang, J.C., and Elgin, S.C. (1984). *Drosophila* DNA topoisomerase I is associated with transcriptionally active regions of the genome. *Proc. Natl. Acad. Sci. USA* **81**, 6958–6962.
- Fuda, N.J., Ardehali, M.B., and Lis, J.T. (2009). Defining mechanisms that regulate RNA polymerase II transcription in vivo. *Nature* **461**, 186–192.
- Gilchrist, D.A., Nechaev, S., Lee, C., Ghosh, S.K., Collins, J.B., Li, L., Gilmour, D.S., and Adelman, K. (2008). NELF-mediated stalling of Pol II can enhance gene expression by blocking promoter-proximal nucleosome assembly. *Genes Dev.* **22**, 1921–1933.
- Gilmour, D.S. (2009). Promoter proximal pausing on genes in metazoans. *Chromosoma* **118**, 1–10.
- Gilmour, D.S., Pflugfelder, G., Wang, J.C., and Lis, J.T. (1986). Topoisomerase I interacts with transcribed regions in *Drosophila* cells. *Cell* **44**, 401–407.
- Guertin, M.J., and Lis, J.T. (2010). Chromatin landscape dictates HSF binding to target DNA elements. *PLoS Genet.* **6**, e1001114.
- Hager, G.L., McNally, J.G., and Misteli, T. (2009). Transcription dynamics. *Mol. Cell* **35**, 741–753.
- Jamrich, M., Greenleaf, A.L., and Bautz, E.K. (1977). Localization of RNA polymerase in polytene chromosomes of *Drosophila melanogaster*. *Proc. Natl. Acad. Sci. USA* **74**, 2079–2083.
- Kaplan, C.D., Morris, J.R., Wu, C., and Winston, F. (2000). Spt5 and spt6 are associated with active transcription and have characteristics of general elongation factors in *D. melanogaster*. *Genes Dev.* **14**, 2623–2634.
- Kraus, W.L., and Lis, J.T. (2003). PARP goes transcription. *Cell* **113**, 677–683.
- Kroeger, P.E., and Rowe, T.C. (1992). Analysis of topoisomerase I and II cleavage sites on the *Drosophila* actin and Hsp70 heat shock genes. *Biochemistry* **31**, 2492–2501.
- Lebedeva, L.A., Nabirochkina, E.N., Kurshakova, M.M., Robert, F., Krasnov, A.N., Evgen'ev, M.B., Kadonaga, J.T., Georgieva, S.G., and Tora, L. (2005).

- Occupancy of the *Drosophila* hsp70 promoter by a subset of basal transcription factors diminishes upon transcriptional activation. *Proc. Natl. Acad. Sci. USA* 102, 18087–18092.
- Lis, J.T. (2007). Imaging *Drosophila* gene activation and polymerase pausing in vivo. *Nature* 450, 198–202.
- Lis, J., and Wu, C. (1993). Protein traffic on the heat shock promoter: parking, stalling, and trucking along. *Cell* 74, 1–4.
- Lis, J.T., Mason, P., Peng, J., Price, D.H., and Werner, J. (2000). P-TEFb kinase recruitment and function at heat shock loci. *Genes Dev.* 14, 792–803.
- Madden, K.R., Stewart, L., and Champoux, J.J. (1995). Preferential binding of human topoisomerase I to superhelical DNA. *EMBO J.* 14, 5399–5409.
- Marshall, N.F., Peng, J., Xie, Z., and Price, D.H. (1996). Control of RNA polymerase II elongation potential by a novel carboxyl-terminal domain kinase. *J. Biol. Chem.* 271, 27176–27183.
- Muller, M.T., Pfund, W.P., Mehta, V.B., and Trask, D.K. (1985). Eukaryotic type I topoisomerase is enriched in the nucleolus and catalytically active on ribosomal DNA. *EMBO J.* 4, 1237–1243.
- Ni, Z., Saunders, A., Fuda, N.J., Yao, J., Suarez, J.R., Webb, W.W., and Lis, J.T. (2008). P-TEFb is critical for the maturation of RNA polymerase II into productive elongation in vivo. *Mol. Cell. Biol.* 28, 1161–1170.
- O'Brien, T., and Lis, J.T. (1993). Rapid changes in *Drosophila* transcription after an instantaneous heat shock. *Mol. Cell. Biol.* 13, 3456–3463.
- Perisic, O., Xiao, H., and Lis, J.T. (1989). Stable binding of *Drosophila* heat shock factor to head-to-head and tail-to-tail repeats of a conserved 5 bp recognition unit. *Cell* 59, 797–806.
- Peterlin, B.M., and Price, D.H. (2006). Controlling the elongation phase of transcription with P-TEFb. *Mol. Cell* 23, 297–305.
- Petes, S.J., and Lis, J.T. (2008). Rapid, transcription-independent loss of nucleosomes over a large chromatin domain at Hsp70 loci. *Cell* 134, 74–84.
- Ritossa, F.A. (1962). A new puffing pattern induced by temperature shock and DNP in *Drosophila*. *Experientia* 18, 571–573.
- Rougvié, A.E., and Lis, J.T. (1988). The RNA polymerase II molecule at the 5' end of the uninduced hsp70 gene of *D. melanogaster* is transcriptionally engaged. *Cell* 54, 795–804.
- Saunders, A., Werner, J., Andrusis, E.D., Nakayama, T., Hirose, S., Reinberg, D., and Lis, J.T. (2003). Tracking FACT and the RNA polymerase II elongation complex through chromatin in vivo. *Science* 301, 1094–1096.
- Saunders, A., Core, L.J., and Lis, J.T. (2006). Breaking barriers to transcription elongation. *Nat. Rev. Mol. Cell Biol.* 7, 557–567.
- Shopland, L.S., Hirayoshi, K., Fernandes, M., and Lis, J.T. (1995). HSF access to heat shock elements in vivo depends critically on promoter architecture defined by GAGA factor, TFIID, and RNA polymerase II binding sites. *Genes Dev.* 9, 2756–2769.
- Sprague, B.L., and McNally, J.G. (2005). FRAP analysis of binding: proper and fitting. *Trends Cell Biol.* 15, 84–91.
- Sprague, B.L., Pego, R.L., Stavreva, D.A., and McNally, J.G. (2004). Analysis of binding reactions by fluorescence recovery after photobleaching. *Biophys. J.* 86, 3473–3495.
- Tsukiyama, T., Becker, P.B., and Wu, C. (1994). ATP-dependent nucleosome disruption at a heat-shock promoter mediated by binding of GAGA transcription factor. *Nature* 367, 525–532.
- Tulin, A., and Spradling, A. (2003). Chromatin loosening by poly(ADP)-ribose polymerase (PARP) at *Drosophila* puff loci. *Science* 299, 560–562.
- García Soriano, F., Virág, L., Jagtap, P., Szabó, E., Mabley, J.G., Liaudet, L., Marton, A., Hoyt, D.G., Murthy, K.G., Salzman, A.L., et al. (2001). Diabetic endothelial dysfunction: the role of poly(ADP-ribose) polymerase activation. *Nat. Med.* 7, 108–113.
- Wang, J.C. (2002). Cellular roles of DNA topoisomerases: a molecular perspective. *Nat. Rev. Mol. Cell Biol.* 3, 430–440.
- Westwood, J.T., Closs, J., and Wu, C. (1991). Stress-induced oligomerization and chromosomal relocalization of heat-shock factor. *Nature* 353, 822–827.
- Yao, J., Munson, K.M., Webb, W.W., and Lis, J.T. (2006). Dynamics of heat shock factor association with native gene loci in living cells. *Nature* 442, 1050–1053.
- Yao, J., Ardehali, M.B., Fecko, C.J., Webb, W.W., and Lis, J.T. (2007). Intracellular distribution and local dynamics of RNA polymerase II during transcription activation. *Mol. Cell* 28, 978–990.
- Yao, J., Zobeck, K.L., Lis, J.T., and Webb, W.W. (2008). Imaging transcription dynamics at endogenous genes in living *Drosophila* tissues. *Methods* 45, 233–241.
- Yoh, S.M., Cho, H., Pickle, L., Evans, R.M., and Jones, K.A. (2007). The Spt6 SH2 domain binds Ser2-P RNAPII to direct Iws1-dependent mRNA splicing and export. *Genes Dev.* 21, 160–174.
- Zhou, M., Halanski, M.A., Radonovich, M.F., Kashanchi, F., Peng, J., Price, D.H., and Brady, J.N. (2000). Tat modifies the activity of CDK9 to phosphorylate serine 5 of the RNA polymerase II carboxyl-terminal domain during human immunodeficiency virus type 1 transcription. *Mol. Cell. Biol.* 20, 5077–5086.